IEEE Sensors Letters Volume 2(3) (2017)
Article Subject (gas sensors)

# Band Gap Engineering of $Pb_{1-x}Cd_xSe$ Thin Films providing mid-IR Photoluminescent Based Light Emitting Diodes for use in Non-Dispersive Infrared Gas Sensors

Greg McGann[1], Carlos Garcia Nuñez[1,2], Lewis Fleming[1,3], David Hutson[1,3], Ewan Waddell,[3] and Des Gibson[1,3]

[1] *Institute of Thin Films, Sensors and Imaging, University of the West of Scotland, SUPA, Paisley PA1 2BE, Scotland, UK*
[2] *University of Glasgow, Glasgow G12 8QQ, Scotland, UK*
[3] *Albasense Ltd, Paisley PA1 2BE, Scotland, UK*

Received 1 Nov 2016, revised 25 Nov 2016, accepted 30 Nov 2016, published 5 Dec 2016, current version 15 Dec 2016. (Dates will be inserted by IEEE; "published" is the date the accepted preprint is posted on IEEE Xplore®; "current version" is the date the typeset version is posted on Xplore®).

**Abstract—** This work describes band-gap engineering of PbCdSe thin films for their use as light emitters in methane gas sensors. $Pb_{0.9}Cd_{0.1}Se$ thin films were synthesized by pulsed direct current (DC) magnetron sputtering. Optical characterisation of films demonstrated successful emission of light at 3.32 μm. Post-sensitization (PS) - in highly reactive oxygen and iodine environment - was also analysed. Design of Experiments (DoE) was used to optimize photoluminescence (PL) of PbCdSe films as a function of PS conditions. The studies demonstrated a high influence of PS temperature on PL properties. The thickness of the films was also demonstrated to have a significant effect on the enhancement of PL. The analysis of the morphology revealed that recrystallisation of the material was key for the emission of light, probing its applicability as mid-IR light source in non-dispersive IR gas sensors.

**Index Terms—** Gas sensors, PbCdSe, mid-IR light source, sputtering

## I. INTRODUCTION

Non-dispersive infrared (NDIR) sensors are based on mid-IR absorption spectroscopy [1], and have demonstrated great potential in extensive applications [2]. NDIR sensors provide benefits such as low cost, high sensitivity, and great integration as a miniaturized sensor configuration compared to other optical-based gas-sensing techniques such as tunable diode laser absorption spectroscopy [3], and photoacoustic spectroscopy [4]. Moreover, NDIR sensors are emerging as a replacement for chemical-based gas sensors [5], addressing inherent problems such as short lifespan, high power consumption, and susceptibility to gas poisoning.

Mid-IR sources are conventionally based on III-V [1], and IV-VI materials [6]. IV-VI semiconductors are preferable for an IR light source/detector over III-V, due to the valence band of IV-VIs is not degenerated, leading to much lower nonradiative Auger recombination in IV-VI [7] than in narrow band-gap III-V semiconductors [8]. Within IV-VI materials, PbSe and CdSe highlight due to their direct band gap and narrow optical band gap energies ($E_g$) of 0.27 eV ($\lambda$ = 4.59 μm) [9] and 1.7 eV ($\lambda$ = 0.729 μm) [10], respectively. These optoelectronic properties make them excellent candidates for the detection of $CO_2$ and $CH_4$, showing high absorption peaks at $\lambda$ of 4.28 μm, and 3.3 μm, respectively [11]. Whilst PbSe has demonstrated great potential for the detection of $CO_2$ [12], the detection of $CH_4$ requires a complex band gap engineering. To that end, one of the most promising methods is the synthesis of ternary compounds, e.g., $Pb_{1-x}Cd_xSe$, where Cd element content decreases the $\lambda$ from 4.59 μm (pure PbSe) down to 3.3 μm (pure CdSe). $Pb_{1-x}Cd_xSe$ thin films with different Cd contents have been successfully deposited by molecular beam epitaxy (MBE) [13], chemical bath deposition [14], and thermal evaporation [15]. Thermal evaporated $Pb_{0.9}Cd_{0.1}Se$ polycrystalline films, exhibiting photoluminescent (PL) emission when films were subjected to an activating annealing in oxygen-containing atmosphere in the presence of iodine vapor. However, this technique showed drawbacks such as low reproducibility, and poor control over PL peak spectral position.

Enhancement of PL emission was already proposed and demonstrated in binary compounds (e.g., PbSe), where the crystal structure improvement was confirmed to be essential for the luminescence of the films [16]. In ternary allows (e.g., $Pb_{1-x}Cd_xSe$) not only the improvement of the crystal structure led to the PL enhancement but also the graded-gap produced by the variation of Cd content along the crystal bulk [15], [17].

In this work, critical wavelength of $Pb_{1-x}Cd_xSe$ semiconductor thin films was firstly theoretically modelled to obtain the $x$ required for PL emission of films at 3.3 μm. Then, films were deposited by sputtering technique, adjusting the concentration of Cd to the modelled value. Design of experiments (DoE) was carried out to evaluate the influence of film thickness and oxygen post-sensitization parameters on the resulting spectral PL of the films. Reproducibility of the method and uniformity of the resulting films were also analysed and evaluated.

Corresponding author: D. Gibson (des.gibson@uws.ac.uk). Carlos Garcia Nuñez, Lewis Fleming and Greg McGann contributed equally.

Digital Object Identifier: 10.1109/LSEN.XXXX.XXXXXXX (inserted by IEEE).

## II. ESTIMATION OF BANDGAP AND COMPOSITION

The estimation of the Cd mass percent (expressed here as $x$) needed to obtain a particular band gap energy in the $Pb_{1-x}Cd_xSe$ material could be calculated using the Bowing's expression [18]:

$$E_g(x, E_{g,PbSe}, E_{g,PbCd}) = (1-x)E_{g,PbSe} + xE_{g,CdSe} - x(1-x)b \quad (1)$$

Where $b$ is the Bowing's constant, and $E_{g,PbSe}$ and $E_{g,CdSe}$ are the band gap energies of the pure binary compounds and calculated considering the temperature dependence of $E_g$ through Varshini's expression [19]:

$$E_g(T, E_{g0}, \alpha, \beta) = E_{g0} - \frac{\alpha T^2}{10^3(T+\beta)} \quad (2)$$

Where $\alpha$ and $\beta$ are Varshini's parameters ($\alpha_{PbSe}$ = -0.515, $\beta_{PbSe}$ = 10, $\alpha_{CdSe}$ = -0.696, $\beta_{CdSe}$ = 281), $T$ is the temperature (expressed in K), and $E_{g0}$ is the band gap of the material at $T$ = 0 K [20]. For a $T$ = 298 K, one gets $E_{g,PbSe}$ of 0.296 eV and $E_{g,CdSe}$ of 1.874 eV. Then, expression (1) is used to fit the experimental data, obtaining a $b$ of 0.9. The resulting graph is used here to optimize the $Pb_{1-x}Cd_xSe$ PL emission at 3.3 µm (0.376 eV), selecting a $x$ of 0.1 (i.e., 10% of Cd) exhibiting a $E_g$ of around 0.39 µm being close to the desirable wavelength.

## III. MATERIALS AND METHODS

### A. Thin Film Deposition

$Pb_{0.9}Cd_{0.1}Se$ thin films were deposited on glass slides (L4242, from Agar Scientific) by pulsed DC magnetron sputtering from a PbSe-CdSe target (80% PbSe - 20% CdSe, from Testbourne Ltd.), using Ar and $O_2$ as process and reactive gases, respectively. The residual pressure before the deposition was 0.67 Pa, 0.40 Pa being the pressure measured during the depositions. The films were deposited at a growth rate of 0.56 nm/s, achieved using Ar flow of 170 sccm, $O_2$ flows of 1 sccm, power of 120 W, pulse width of 5 ms, and pulse frequency of 50 kHz (10 kW power supply from Advanced Energy Pinnacle+). No intentional substrate heating was implemented.

### B. Post-sensitization

After the deposition, PbCdSe thin films were loaded in a tube furnace and exposed to an $O_2/N_2$ ambient (2 lpm for both gases) in a borosilicate reaction vessel for the sensitization process for 60 and 105 min and at temperatures of 450 and 550 ºC.

### C. Material Characterisation

Figure 1(a) presents a schematic of the setup developed here to characterize the optical properties of PbCdSe films. An IR light-emitting diode (LED) with a wavelength ($\lambda$) of 850 nm (i.e., 1.46 eV) was used to irradiate the samples. For that, an electronic driver – connected to a wave function generator (WFG) – was utilised to power the LED using a pulse function with a certain amplitude and frequency. The frequency of the pulsed light emitted by the LED was utilised as a trigger input in an oscilloscope (Figure 1(a)). The driver signal was monitored as a reference in the channel 2 (CH2) of the oscilloscope. Pulsed LED light was transmitted through the sample (including transparent glass substrate and PbCdSe film). The energy of the incident photons was enough to excite electrons from valence band (VC) to the conduction band (CB) (Figure 1(b)). Right after,

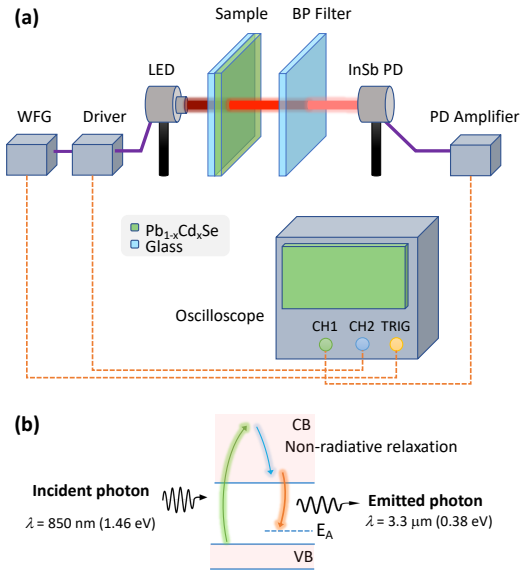


Figure 1. Schematic diagrams of (a) PL characterisation system and (b) PL working principle.

excited electrons show a non-radiative relaxation within the CB. Finally, electron-hole recombination between CB and the acceptor level ($E_A$) introduced by the oxygen defects during the sensitization step occurs, leading to the emission of a photon with an energy equal to $E_g$-$E_A$. In our setup, a band-pass (BP) filter is used to filter out all the photons emitted by PbCdSe films with $\lambda \neq 3.3$ µm (i.e., 0.376 eV). The filtered light is then collected by a PD whose signal is amplified and displayed in the channel 1 (CH1) of the oscilloscope.

The PL emission properties of the films were characterised by using an adapted Fourier transform infrared (FTIR) spectroscopic system (Nicolet iS50, from Thermo Fisher Scientific) at λ ranged between 2 to 5 µm. Morphological properties of the films *before* and *after* the oxygen sensitization were analysed by scanning electron microscopy (SEM) at 20 kV (S4100 cold FEG 101 from Hitachi).

### D. Design of Experiments (DoE)

A 2-factor full factorial design with 2 levels for each factor was generated using RStudio. Process variables comprised film thickness (700 and 1000 nm), post-sensitization time (60 and 105 min), and post-sensitization temperature (450 and 550 ºC). The $2^k$ runs were generated with $k$ = 3, where $k$ is the number of factors, yielding 8 runs in total. The DoE with PL response was re-imported back into RStudio and the results were fit to a linear model. Half normal, main effects, and interactions plots for PL were generated and analyzed.

## IV. RESULTS AND DISCUSSION

### A. Morphological Characterization

Figure 2 summarizes the main results obtained from the morphological characterisation of $Pb_{0.9}Cd_{0.1}Se$ films deposited at 0-sccm (Figure 2(a)) and 1-sccm (Figure 2(b)) of $O_2$ flux, and after their post-sensitization (Figure 2(c) and (d), respectively). SEM image of films deposited in absence of $O_2$ clearly evidences a polycrystalline morphology, with a high density of pyramid-like nanostructures (*see* inset of Figure 2(a)) covering uniformly the entire area of the substrate.

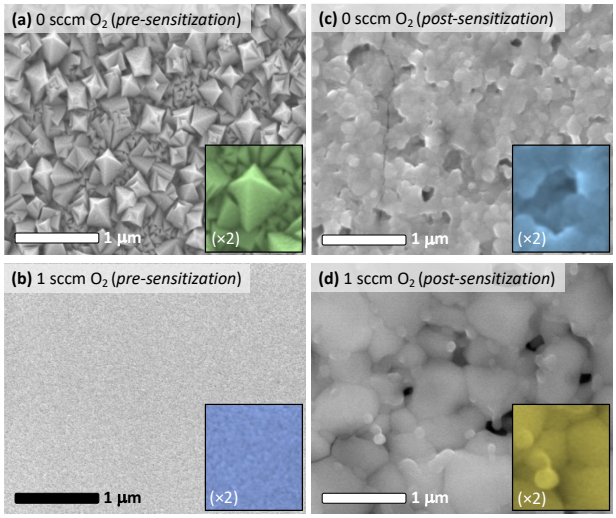


Figure 2. SEM images of $Pb_{0.9}Cd_{0.1}Se$ films deposited @ (a) 0-sccm and (b) 1-sccm $O_2$ flux; insets: ×2 zoom-in SEM images. (c,d) SEM images of post-sensitized $Pb_{0.9}Cd_{0.1}Se$ films.

This result is in good agreement with previous works reported in the literature [15], [21] where microstructures with the shape of pyramids at the surface of thermally evaporated $Pb_{0.9}Cd_{0.1}Se$ films were also observed prior to the sensitization step. The effect of the post-sensitization – in a $O_2$ reactive environment – was also analysed by SEM, demonstrating a drastic effect on the film morphology. As observed in Figure 2(c), nano-pyramids transform into a less rough morphology, with 'blurry' boundaries between grains/domains compared to the as-deposited film (*see* inset of Figure 2(a)). One could also observe that the size of the domains is preserved upon the post-sensitization (*see* inset of Figure 2(c)), agreeing literature results for this material [15], [21]. The change in the morphology is associated to the recrystallization of the film surface induced by the iodine vapor during the annealing step, as confirm cross-section SEM images reported elsewhere [15]. This recrystallisation has been also confirmed by XRD measurements, where new phases, including lead oxides, lead iodides, and cadmium iodides, are also formed [15].

## B. Optical Characterization

The study of the PL in $Pb_{0.9}Cd_{0.1}Se$ thin films deposited with and without oxygen, concluded that $O_2$ is essential for the observation of PL in these films. This result is in good agreement with the literature [15], where $Pb_{0.9}Cd_{0.1}Se$ films only presented PL emission after their activation in an oxygen-containing atmosphere. Figure 3(a) shows the PL peak of three samples deposited under the same conditions (Figure 2(d)), i.e., a $Pb_{0.9}Cd_{0.1}Se$ thin films deposited under 1-sccm $O_2$ flux and post-sensitized. From that graph, one could conclude that the creation of oxygen defects levels in the PbCdSe band structure due to the sensitization process [22], leads to the emission of light at $\lambda$ of around 3.32 µm. Moreover, the graph confirms the high level of reproducibility of the sputtering procedure presented here, exhibiting a PL peak well-centered around 3.32 µm for the three growth runs (<0.5% peak position spread). For the sake of comparison, three $Pb_{0.9}Cd_{0.1}Se$ thin films deposited by thermal evaporation [17] have

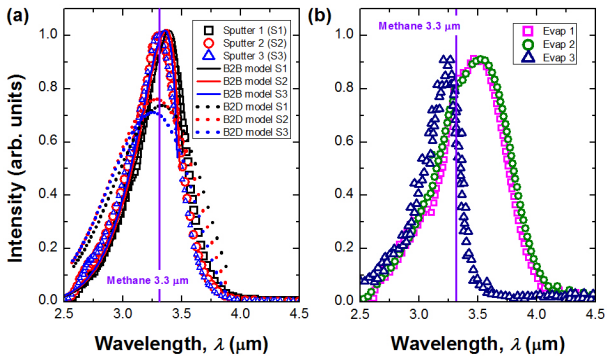


Figure 3. PL response vs wavelength of $Pb_{0.9}Cd_{0.1}Se$ films deposited by (a) sputtering (under 1-sccm $O_2$ flux and post-sensitized) and (b) by thermal evaporation [17]. (a) Experimental results represented along with B2B (*straight lines*) and B2D models (*dotted lines*).

been also characterized under the same conditions (Figure 3(b)). The optical characterization of the films concludes that evaporation lacks control on doping level as evident from the PL peak shift between growth runs (>4% peak position spread). In addition, evaporation presents a poor tunability of the band gap, resulting in a misalignment of the emission wavelength out of the desirable value (around 3.3 µm). Finally, comparing Figure 3(a) and (b) one could also observe that sputtered films present a PL peak with less bandwidth, which is beneficial from the optical point of view in the design of NDIR based gas sensors. For the sake of completion, the three samples of Figure 3(a) have also been analyzed by energy dispersive X-ray (EDX) analysis, confirming the good agreement of the composition not only of the three samples but also the lateral uniformity of resulting films.

Figure 3(a) also presents the experimental results along with simulations calculated using both direct band-to-band (B2B) transition and band-to-deep (B2D) level model [23]. The simulations still do not confirm a main mechanism governing the PL of PbCdSe, B2B and B2D reproducing better the lower and higher energy edges of the PL peak, respectively. Previous works reported in the literature indicate that B2D fits better the experimental results [17], which might suggest the evaporation technique induces the accumulation of charge carriers generated by the excitation radiation in the parts of nano-crystallites with the narrowest band gap, and also the formation of the graded-gap structure in the grain bulk.

To further understand the role of the post-sensitization conditions on the optical properties of PbCdSe films, a first interaction full factorial DoE using RStudio was employed here. For that, key input variables (KIVs) included post-sensitization (PS) time and temperature, and the thickness of the film. KIVs along with the key output variable (KOVs), i.e., PL intensity observed at $\lambda = 3.3$ µm, as summarized in Table 1. KOV demonstrated that post-sensitization temperature is the parameter exhibiting a significant influence on the resulting PL intensity. For the sake of clarity, Figure 4 presents the half normal plot, where the significant effect of PS temperature is clearly observed. A second DoE interaction carried out at higher PS temperatures (550 and 575 °C) was carried out to further optimize the PL response of PbCdSe films. For that, the other two KIV were the thickness (1 and 1.3 µm) and the PS time (45 and 75 min). At high PS temperatures - thickness is the most significant parameter on the PL

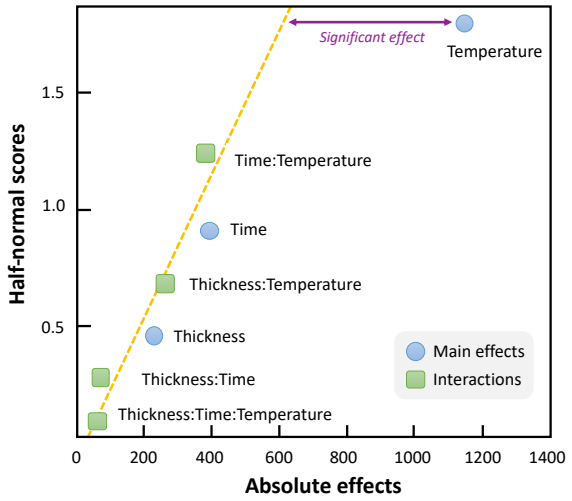


Figure 4. DoE results (1st interaction) describing the main effects and interactions of film thickness, annealing time, and annealing temperature on the PL response of the PbCdSe films.

properties of the films. In those conditions, a thickness of 1.3 µm produced a factor 2 improvement in the resulting PL of the films. This result is attributed to the existence of well-established and efficient recombination pathways within thicker PbCdSe films [30].

## V. CONCLUSION

This work presents a novel PbCdSe thin film deposited by pulsed DC magnetron sputtering, exhibiting reproducible light emission at mid-IR wave band, aligned with use as a low cost and mass producible light source for NDIR gas sensors. PL measurements demonstrated sensitization of PbCdSe films was essential to exhibit a PL peak at around methane gas absorptance (3.32 µm). This result demonstrated the successful band-gap engineering of the $Pb_{0.9}Cd_{0.1}Se$ films producing light in the electromagnetic wave band range required for methane gas detection. Moreover, sputtering technique was confirmed to produce a reproducible PL peak centered around 3.3 µm, in various PbCdSe films deposited under the same conditions. DoE also probed high influence of PS temperatures at thinner samples, and the significant influence of the film thickness for samples PS at higher temperatures and for shorter times.

Table 1. DoE results (1st interaction) of post-sensitization of PbCdSe films.

| DoE | Thickness (nm) | PS time (min) | PS [a] temperature (°C) | PL [b] (mV) |
|---|---|---|---|---|
| 1 | 700 | 105 | 550 | 688 |
| 2 | 1,000 | 105 | 450 | 80 |
| 3 | 1,000 | 105 | 550 | 1,060 |
| 4 | 1,000 | 60 | 550 | 1,940 |
| 5 | 1,000 | 60 | 450 | 92 |
| 6 | 700 | 60 | 450 | 116 |
| 7 | 700 | 60 | 550 | 1,340 |
| 8 | 700 | 105 | 450 | 136 |

[a] Post-sensitization: PS; [b] Photoluminescence: PL.

## ACKNOWLEDGMENT

This work was supported in part by InnovateUK (10034903) and UWS Vice Chancellor Fellowship. Authors also thank West of Scotland Science Park (Glasgow, UK) for the PL spectral measurements.

## REFERENCES

[1] D. Gibson and C. MacGregor, "A Novel Solid State Non-Dispersive Infrared CO2 Gas Sensor Compatible with Wireless and Portable Deployment," *Sensors 2013, Vol. 13, Pages 7079-7103*, vol. 13, no. 6, pp. 7079–7103, 2013.

[2] R. K. Jha, "Non-Dispersive Infrared Gas Sensing Technology: A Review," *IEEE Sens J*, vol. 22, no. 1, pp. 6–15, 2022.

[3] G. M. Ma *et al.*, "Tracing Acetylene Dissolved in Transformer Oil by Tunable Diode Laser Absorption Spectrum," *Scientific Reports 2017 7:1*, vol. 7, no. 1, pp. 1–8, 2017.

[4] M. Baptista-Filho *et al.*, "Ammonia traces detection based on photoacoustic spectroscopy for evaluating ammonia volatization from natural zeolites at typical crop field temperature," *Sens Actuators B Chem*, vol. 158, no. 1, pp. 241–245, 2011.

[5] E. Bakker and M. Telting-Diaz, "Electrochemical sensors," *Anal Chem*, vol. 74, no. 12, pp. 2781–2800, 2002.

[6] J. S. Sanghera, L. B. Shaw, and I. D. Aggarwal, "Chalcogenide glass-fiber-based mid-IR sources and applications," *IEEE Journal on Selected Topics in Quantum Electronics*, vol. 15, no. 1, pp. 114–119, 2009.

[7] P. C. Findlay *et al.*, "Auger recombination dynamics of lead salts under picosecond free-electron-laser excitation," *Phys Rev B*, vol. 58, no. 19, p. 12908, 1998.

[8] J. R. Meyer *et al.*, "Auger coefficients in type-II InAs/Ga1−xInxSb quantum wells," *Appl Phys Lett*, vol. 73, no. 20, pp. 2857–2859, Nov. 1998.

[9] V. Arivazhagan, M. Manonmani Parvathi, and S. Rajesh, "Impact of thickness on vacuum deposited PbSe thin films," *Vacuum*, vol. 86, no. 8, pp. 1092–1096, 2012.

[10] R. B. Kale and C. D. Lokhande, "Systematic study on structural phase behavior of CdSe thin films," *Journal of Physical Chemistry B*, vol. 109, no. 43, pp. 20288–20294, 2005.

[11] M. Ando, H. Kawasaki, S. Tamura, Y. Haramoto, and Y. Shigeri, "Recent Advances in Gas Sensing Technology Using Non-Oxide II-VI Semiconductors CdS, CdSe, and CdTe," *Chemosensors 2022, Vol. 10, Page 482*, vol. 10, no. 11, p. 482, 2022.

[12] M. M. A. & F. S. M. Ibtehal F. Mahdi*, "Measurement of Carbon Dioxide Concentration using Pbse Detector," *Journal of Optoelectronics Laser*, vol. 41, no. 9, pp. 54–63, Sep. 2022, Accessed: Jun. 29, 2023.

[13] S. Chusnutdinow *et al.*, "Ternary Pb1−xCdxSe films grown by molecular beam epitaxy on GaAs/ZnTe hybrid substrates," *J Cryst Growth*, vol. 507, pp. 10–15, 2019.

[14] E. V. Maraeva, A. A. Shupta, A. A. Bobkov, V. S. Levitskii, A. I. Maximov, and V. A. Moshnikov, "The photoluminescence and phase composition of lead sulphide–cadmium sulphide layers obtained by chemical bath deposition," *J Phys Conf Ser*, vol. 735, no. 1, p. 012056, 2016.

[15] A. E. Gamarts, V. A. Moshnikov, and D. B. Chesnokova, "Photoluminescence in the Pb1-x CdxSe polycrystalline layers activated in the presence of iodine vapor," *Semiconductors*, vol. 40, no. 6, pp. 662–664, Jun. 2006.

[16] N. P. Anisimova, N. E. Tropina, and A. N. Tropin, "Enhancement of the output emission efficiency of thin-film photoluminescence composite structures based on PbSe," *Semiconductors*, vol. 44, no. 12, pp. 1554–1558, 2010.

[17] D. B. Chesnokova, V. A. Moshnikov, A. E. Gamarts, E. V. Maraeva, O. A. Aleksandrova, and V. V. Kuznetsov, "Structural characteristics and photoluminescence of Pb1 − xCdxSe (x = 0–0.20) layers," *J Non Cryst Solids*, vol. 356, no. 37–40, pp. 2010–2014, Aug. 2010.

[18] J. D. Gallagher, C. L. Senaratne, J. Kouvetakis, and J. Menéndez, "Compositional dependence of the bowing parameter for the direct and indirect band gaps in Ge1-ySny alloys," *Appl Phys Lett*, vol. 105, no. 14, p. 142102, 2014.

[19] R. O. Ocaya, "Thermal tuning of light-emitting diode wavelength as an implication of the Varshni equation," *Measurement*, vol. 162, p. 107910, 2020.

[20] O. (Otfried) Madelung, "Semiconductors. Group IV elements and III-V compounds," p. 164, 1991, 2023.

[21] M. Hazra and J. Datta, "Optimal Blending of PbSe and CdSe in Polycrystalline PbCdSe Nanocomposite Film: Improved Carrier Multiplication and Enhanced Photoconversion Efficiency," *ACS Appl Mater Interfaces*, vol. 11, no. 43, pp. 40393–40405, 2019.

[22] A. Alkauskas, M. D. McCluskey, and C. G. Van De Walle, "Tutorial: Defects in semiconductors - Combining experiment and theory," *J Appl Phys*, vol. 119, no. 18, p. 181101, 2016.

[23] G. Lucovsky, "On the photoionization of deep impurity centers in semiconductors," *Solid State Commun*, vol. 3, no. 9, pp. 299–302, 1965.